Pergamon

Geochimica et Cosmochimica Acta, Vol. 68, No. 22, pp. 4649-4663, 2004

0016-7037/04 $30.00 + .00

doi:10.1016/j.gca.2004.04.022

Lead and strontium isotopes as monitors of experimental granitoid mineral dissolution

YIGAL EREL,[1,*] JOEL D. BLUM,[2] EMMANUELLE ROUEFF,[3] and JIWCHAR GANOR[3]

[1]Institute of Earth Sciences, The Hebrew University of Jerusalem 91904, Jerusalem, Israel
[2]Department of Geological Sciences, The University of Michigan, Ann Arbor, MI 48109, USA
[3]Department of Geological and Environmental Sciences, Ben-Gurion University, Beer Sheva 84105, Israel

(*Received December* 1, 2003; *accepted in revised form April* 21, 2004)

Abstract—Flow-through dissolution experiments were carried out on crushed granitoid rock (the Elat Granite) and three mineral separates (plagioclase, perthite, and biotite + chlorite) from this rock at pH 1 and 25°C. Major element concentrations were combined with Pb and Sr isotopic analyses of starting materials and output solutions and together enabled us to elucidate several important mechanisms related to granitoid rock weathering. We observed an initial stage of rock dissolution (<200 hours of reaction) that was characterized by elemental release from traces of calcite and/or apatite and to a lesser extent from the interlayer sites of biotite. Dissolution in the interval of 200 to 400 h was dominated by the release of elements from the interlayer sites of biotite, and at 400 to 1000 h of reaction the chemistry of output solutions was dominated by the release of elements from tetrahedral and octahedral sites of biotite as well as from plagioclase. After 1000 h, the dissolution of plagioclase, and to a lesser extent biotite, dominated the composition of elements released by the rock. We demonstrate that Pb and Sr isotope ratios in the output solutions can be used to identify each of these stages of dissolution. By comparing our experimental results on the release of Pb and Sr isotopes with field measurements of Pb and Sr isotopes in soil chronosequences from the Wind River and the Sierra Nevada Mountains (USA), we are able to show that similar isotopic patterns appear in both the pH 1 experiments and in soils formed under natural conditions at higher pH. By combining these experimental results with previous field studies, we are able to estimate the duration of most of these stages of granitoid weathering under natural conditions in temperate climates. In soils older than a few hundred years and younger than 10,000 yr the release of elements from interlayer sites of biotite controls the weathering flux. Soils between 10,000 and 100,000 yr old are dominated by biotite and plagioclase weathering, with biotite weathering controlling the first part of this period and plagioclase dominating the later part. After more than 100,000 yr, plagioclase, and to a lesser degree biotite, dominate the weathering flux within these granitoid soils. *Copyright © 2004 Elsevier Ltd*

1. INTRODUCTION

The study of rock and mineral dissolution rates has been a major theme in low-temperature geochemical research for many years. This is due in large part to the fact that mineral dissolution controls the release of both nutrient and toxic elements to soils and to the hydrocycle, and ultimately exerts an important control on the composition of the oceans and atmosphere. In recent years, a few studies have integrated the measurements of Sr and Pb isotopes in laboratory dissolution experiments yielding new information on (1) the importance of accessory mineral inclusions in what were previously considered "pure" mineral starting materials, (2) the differential rate of release of cations from contrasting mineralogic sites within single minerals, and (3) the relative rates of weathering of minerals in multi-mineral dissolution experiments (Bullen et al., 1997, 1998; Brantley et al., 1998; White et al., 1999; Taylor et al., 2000a,b; Harlavan and Erel, 2002; Blum and Erel, 2003).

In general, the age and the ratios of radioactive parent to daughter elements such as Rb/Sr, U/Pb, and Th/Pb in minerals determine their $^{87}Sr/^{86}Sr$, $^{206}Pb/^{204}Pb$, $^{207}Pb/^{204}Pb$, and $^{208}Pb/^{204}Pb$ values. Therefore, the isotopic composition of Sr and Pb in the weathering products can be used to characterize the minerals that are weathering. For example, elevated $^{206}Pb/^{204}Pb$ and $^{207}Pb/^{204}Pb$ values in solution suggest that urogenic (U-enriched) minerals such as apatite are preferentially being weathered, elevated $^{208}Pb/^{204}Pb$ values suggest that thorogenic minerals such as monazite are being weathered, and elevated $^{87}Sr/^{86}Sr$ values suggest that rubidium-rich minerals such as biotite are being weathered.

Using Sr isotopes, it was demonstrated that Sr release to solution from reacting minerals is not congruent with respect to major element concentrations (White et al., 1999). It was proposed that this was due either to the extreme sensitivity of Sr isotope ratios to the dissolution of trace Ca-bearing phases with low $^{87}Sr/^{86}Sr$, the preferential retention of Sr relative to K in biotite, or the preferential leaching of Sr with low $^{87}Sr/^{86}Sr$ from plagioclase or K-feldspar. White et al. (1999) also suggested that $^{87}Sr/^{86}Sr$ ratios derived from granitoid weathering might be temperature dependent, with somewhat lower ratios released in warmer climates.

Similarly, Brantley et al. (1998) observed that during the dissolution of bytownite, microcline, and albite, Sr release early in the experiments was neither stoichiometric nor isotopically the same as the bulk mineral and could be attributed to the dissolution of mineral inclusions in the feldspars and/or to leaching of cations from mineral defect sites. Once the dissolution of these minerals reaches a steady state, however, the $^{87}Sr/^{86}Sr$ ratio released to solution becomes equal to the bulk material.

The dissolution kinetics and Sr release from biotite, phlogo-

* Author to whom correspondence should be addressed (yerel@vms.huji.ac.il).

Table 1. Elemental composition and isotopic ratios of the mineral separates, whole rock, and hypothetical whole rock.

	Biotite + chlorite–rich[a]	Quartz-rich	Plagioclase-rich	Perthite-rich	Whole rock	Hypoth. rock[b]
SiO_2	40	91	66	66	76	74
Al_2O_3	18	5.2	19.7	19.4	14.0	14.5
FeO	22	0.07	0.2	0.1	1.4	1.1
TiO_2	2.0	0.01	0.01	0.01	0.12	0.10
CaO	1.4	0.59	1.6	0.29	0.96	0.97
MgO	3.5	0.02	0.03	0.01	0.20	0.17
MnO	0.49	0.00	0.01	0.01	0.03	0.03
Na_2O	1.5	2.05	7.4	3.3	4.0	4.4
K_2O	3.8	0.33	2.5	10.0	3.4	3.4
P_2O_5	0.2	0.020	0.040	0.020	0.06	0.04
[Pb]	35	3.7	12	27	15.3	14.2
[Sr]	35	38	110	90	65	76
[U]	8.6	0.38	0.23	0.32	1.0	0.7
[Th]	38	0.51	0.34	0.25	9.5	2.1
$^{206}Pb/^{207}Pb$	1.274	1.178	1.151	1.144	1.205	1.15
$^{208}Pb/^{207}Pb$	2.656	2.440	2.436	2.428	2.490	2.45

All oxides are in wt.% in the rock, all trace metals are in ppm.

[a] The composition of the biotite + chlorite–rich fraction was measured before the last stage of the mineral separation.

[b] The hypothetical rock calculations for concentration of elements include all four mineral separates, but the isotopic and elemental ratios were calculated without quartz.

pite, and labradorite were investigated by Taylor et al. (2000a,b) who stressed the importance of trace calcite inclusions in biotite and phlogopite during the early stages of weathering. In addition, a more rapid release of interlayer cations from biotite and phlogopite compared to octahedral and tetrahedral cations was observed, and it was found that labradorite dissolution is congruent, with stoichiometric Sr release unaffected by solution saturation state or preferential release from mineral defect sites. A common theme of all these experimental studies is that trace inclusions of calcite and other nonsilicate phases are common in the silicate mineral specimens that have been used extensively for silicate dissolution experiments, and Sr isotopes are very sensitive to their presence. In the early stages of weathering the $^{87}Sr/^{86}Sr$ ratio of the solutions can differ significantly from that of the bulk mineral, but once a steady state is reached the dissolution of calcite and other inclusions is limited by the rate at which these inclusions are exposed to solutions, due to the dissolution of the host silicate minerals.

Harlavan and Erel (2002) studied the release of Pb and rare earth elements (REE) during the dissolution of crushed granite subjected to sequential batch leaching with dilute acids, and compared the results with Pb and REE data from soils developed on the same bedrock (Harlavan et al., 1998; Harlavan and Erel, 2002). During the early stages of granitoid dissolution, Pb and REE were preferentially released from some of the accessory phases (i.e., allanite, sphene, and apatite) leading to higher $^{206}Pb/^{207}Pb$ and $^{208}Pb/^{207}Pb$ ratios and different REE patterns in solution than in the bulk rock itself. Three stages of rock dissolution were identified based on the isotopic ratios of Pb and the REE patterns. Among the accessory phases, allanite dissolution dominated the first stage, in which $^{208}Pb/^{207}Pb$ ratios in solution increased with soil age and approached the values of allanite. In the second stage, dissolution of apatite and sphene became more significant. In the third stage, the accessory phases were depleted and feldspar dissolution became dominant. Harlavan et al. (1998) also argued that biotite dissolution was significantly more rapid than hornblende under the experimental conditions of dilute acid leaching.

In the present study, the isotopes of Pb and Sr and the concentrations of the major elements released during the dissolution of a granitoid rock and its major minerals are studied together for the first time. By conducting experiments on both whole rock samples and mineral separates from the same rock, we worked to bridge the gap between the information obtained from radiogenic isotope studies of the dissolution of individual minerals in the laboratory, and studies of radiogenic isotopes released from whole rock weathering in natural weathering environments. The present paper discusses the change in isotopic and chemical composition during the dissolution of the Elat Granite. The dissolution rates of this granite and its minerals are discussed in detail by Ganor et al. (in press).

2. EXPERIMENTAL METHODS

The rock used for the dissolution experiments is the Elat Granite from the Nahal Shlomo pluton, which outcrops approximately 5 kilometers southeast of the city of Elat in southern Israel. It is a medium- to coarse-grained granite composed mainly of plagioclase ($An_{12–15}$; 21–28%), perthite with 20–30% albite (30–35%), quartz (34–39%), and biotite (3.5–5.5%) (Eyal et al. 2004). The sample used in the present study was altered by hydrothermal fluids shortly after its formation. As a result, the biotite was partly transformed into chlorite, and feldspars were partly replaced by sericite and are stained red because of Fe-oxide coatings (surface staining). The alteration is on mineral surfaces and in microscopic cracks that cut through the grains.

Minerals were separated from samples of the Elat Granite as follows. Rock samples were crushed in a jaw crusher and then in a disk mill, and the samples were sieved to isolate the 150–250 μm size. Mineral separation was achieved by utilizing contrasts in the densities and magnetic properties of the various minerals. The "heavy liquid" Na-polytungstate was mixed with water to provide a range of liquid densities that bracketed the various minerals. Density separates were then further purified using a Franz isodynamic magnetic separator, and a microscope was used to hand-pick some impurities. This yielded four mineral fractions: plagioclase-rich, perthite-rich, biotite + chlorite–rich, and quartz-rich. Despite our efforts, the mineral separates were not entirely pure (Tables 1 and 2). In addition, a portion of the heavy minerals that were not inclusions in other minerals were lost during the

Table 2. (a) Elemental composition of the major minerals in the rock analyzed with electron microprobe in wt.%. The K-feldspar is the purest endmember that we could analyze within the perthite. (b) Concentrations in ppm and isotope ratios of Sr and Pb in plagioclase, biotite + chlorite, K-feldspar, calcite/apatite used for the hypothetical rock calculations. The isotopic values were obtained from the leaching experiments of the nonpure mineral separates. Sr and Pb (with the exception of Pb in biotite + chlorite) concentrations (ppm) were assumed to be equal to the mineral separates given in Table 1 The value of Pb concentration in the biotite + chlorite pure minerals should be lower than in the mineral separate since these phases contain a large amount of Pb-rich inclusions; nevertheless, the actual value of 10 ppm was chosen in order to maximize the fit between the measured and the calculated $^{206}Pb/^{207}Pb$ values. The values for calcite/apatite were assumed to be similar to the values of plagioclase.

	Plagioclase		K-feldspar		Biotite		Chlorite		Quartz		Muscovite		Apatite	
(a) Element	average	% stdev	average	% stdev	average	% stdev	average	% stdev	average	% stdev	average	% stdev	average	% stdev
SiO_2	65	3%	65	1%	33	4%	23	4%	98	3%	46	3%	0.07	40%
Ti_2O			0.2	125%	2.3	21%	0.2	73%	0.08	102%	0.4	74%	0.04	10%
Al_2O_3	22	3%	19	2%	18	2%	19	4%	0.06	120%	28	10%		
FeO	0.10	117%	0.3	111%	26	8%	36	9%			7.3	17%	0.2	33%
MgO	0.02	0%	0.02	156%	4.2	20%	5.0	8%			1.6	29%	0.03	3%
CaO	2.7	59%	0.09	102%	0.1	81%	0.0	103%	0.01	10%	0.04	134%	54	3%
Na_2O	8.8	16%	1.0	110%	0.3	30%	0.2	23%	0.04	10%	0.2	51%	0.2	27%
K_2O	0.54	51%	16	11%	8.7	12%	0.1	77%	0.02	10%	10	7%	0.1	31%
P_2O_3	0.02	117%	0.02	175%	0.1	217%	0.02	222%	0.10	6%	0.08	116%	38	5%
sum	99	1%	101	2%	93	3%	84	4%	99	3%	94	3%	93	1%

(b)	Plagioclase	K-feldspar	Biotite + chlorite	Calcite/apatite#
$^{206}Pb/^{207}Pb$	1.155	1.144	1.242	1.155
$^{208}Pb/^{207}Pb$	2.408	2.405	2.435	2.408
[Pb]	12	27	10	12
$^{87}Sr/^{86}Sr$	0.710	0.721	0.070	0.710
[Sr]	110	90	35	110

mineral separation process (mostly thorogenic minerals). Aliquots from the rock and mineral separate samples were digested with concentrated HF and HNO_3 for trace metal and isotopic analyses and fused with Li-metaborate and dissolved in dilute HNO_3 for major elemental analysis (Table 1).

The dissolution experiments were conducted under far-from-equilibrium conditions at pH 1 and a temperature of 25°C using ultrapure HNO_3 as the input solution. Experiments were carried out under clean conditions using a newly designed 35-mL "trace-metal clean" flow-through reactor. The reaction cell is a closed cylinder of Lexan plastic that contains an inlet line and a filtered outlet line. A peristaltic pump controls the flow rate through the reaction chamber. Solutions are filtered on the output side of the vessel with a precleaned 0.45-μm membrane. Rock and mineral samples were ground to 75–150 μm diameter grain size, and 2.0–3.0 g in mass was loaded into the flow reactor. Temperature was kept constant with the use of double-walled reactors, through which constant-temperature water flowed. Before each experiment, the cell, filter, and tubes were thoroughly cleaned by flushing with the input solution for several days, and the blank output solutions were analyzed to determine the background levels of major and trace elements. The blank concentrations were usually less than 1% of the lowest output solution concentration during the experiments. In this study, four dissolution experiments were conducted using the whole rock sample and plagioclase-rich, perthite-rich, and biotite + chlorite–rich mineral separates. The whole rock dissolution experiment was conducted for 4200 h, the perthite experiment for 4000 h, the plagioclase experiment for 3000 h, and the biotite + chlorite experiment for 2600 h. The experiments were terminated when the $^{206}Pb/^{207}Pb$ ratio of output solutions reached a constant value. It is very important to note that after 1220 h the sample from the whole rock experiment was taken out of the cell, dried at 50°C, and then the experiment was resumed. The mineral separates did not undergo any drying steps during the dissolution experiments.

Trace elements (P, U, Th, Pb, and Sr) in the rock and mineral digests and in the leaching solutions were analyzed by inductively coupled plasma mass spectrometry (ICP-MS) (Perkin Elmer Elan 6000) after internal standards (Rh and Re) were added. A second aliquot of each solution was analyzed for major elements (Si, Al, Ca, Mg, K, Na, Fe, Ti) by inductively coupled plasma optical emission spectroscopy (Perkin Elmer Optima 3000). The pH of the output solution was measured using a combination electrode. Lead and Sr separation chemistry for isotopic measurement were carried out following the techniques given by Blum et al. (1993) and Erel et al. (1994). Lead isotopic compositions were measured with a multi-collector inductively coupled plasma mass spectrometer (MC-ICP-MS; Nu Instruments MC-ICP-MS). Mass fractionation was closely monitored by frequent analysis of NIST standards under identical running conditions as samples. $^{206}Pb/^{207}Pb$ and $^{208}Pb/^{207}Pb$ ratios were used instead of $^{206}Pb/^{204}Pb$, $^{207}Pb/^{204}Pb$, and $^{208}Pb/^{204}Pb$ because of the low concentrations of Pb in many of our samples, which did not allow precise measurements of ^{204}Pb (^{204}Pb accounts for only 1–2% of the Pb in the sample). The NIST 981 standard was used for Pb isotope calibration and had long-term mean values of: $^{206}Pb/^{207}Pb = 1.0943 \pm 0.0002$ and $^{208}Pb/^{206}Pb = 2.1655 \pm 0.0009$. Mass discrimination was corrected by admixing Tl (50 ppb) into both the NIST 981 standard and the samples. Sr isotopic compositions were determined by a thermal ionization mass spectrometer (TIMS Finnigan MAT 262). $^{87}Sr/^{86}Sr$ ratios were corrected for mass fractionation to $^{86}Sr/^{84}Sr = 0.1194$. The precision of $^{87}Sr/^{86}Sr$ ratios was ± 0.000012 or smaller. Analyses of NIST SRM 987 yielded a mean value of 0.710262 ± 0.000013. Several thin sections of the Elat Granite were carbon-coated and examined with a JEOL JXA-8600 electron microprobe for quantitative chemical analyses of major and minor minerals (Table 2a).

3. RESULTS

The elemental concentrations and isotopic ratios of total digests of the rock and mineral separates (perthite-rich, plagioclase-rich, biotite + chlorite–rich, and quartz-rich) are summarized in Table 1. By comparing the chemical composition of the digested mineral separates with the composition of the minerals in rock thin-sections determined by electron microprobe, it is clear that none of the mineral separates are pure (Tables 1 and 2). For example, the perthite-rich fraction contains ~80% perthite (K-feldspar + albite), ~11% plagioclase (An_{12-15}), and ~6% quartz, while the plagioclase fraction contains ~60% plagioclase, ~32% perthite,

~6% quartz, and <0.5% biotite + chlorite. The biotite + chlorite fraction also contains some quartz and plagioclase as inclusions. In addition, all major minerals contain inclusions of accessory minerals. Plagioclase contains inclusions of muscovite and small monazite and apatite crystals. Perthite contains inclusions of monazite, garnet, apatite, titano-magnetite, and ilmenite. The quartz crystals contain a few inclusions of garnet, monazite, and apatite. The biotite grains contain the largest quantity of inclusions including apatite, zircon, monazite, and ilmenite. Major element concentrations in the output solutions, total digested mineral separates, and whole rock samples were used in a mass balance calculation (outlined in the discussion) to quantify the proportions of each pure major mineral (using the electron microprobe values) in the output solutions of the whole rock and mineral separate experiments (Tables 1–3).

Plagioclase, perthite, and biotite + chlorite contain most of the major cations (and Pb and Sr) in the rock (Table 1) and weather substantially faster than quartz (White and Brantley, 1995); therefore, quartz dissolution was not considered here. The isotopic composition of Pb and Sr released by the dissolution of the three mineral separates (biotite + chlorite–rich, perthite-rich, and plagioclase-rich) are different than the values of the total digest of the mineral separates (Fig. 1, Tables 1 and 3). In addition, the $^{206}Pb/^{207}Pb$ values of perthite-rich, and plagioclase-rich mineral separates decrease with time, approaching the total digested values after more than 3000 h of leaching. It is interesting to note that at this time, Fe, probably released from the Fe-oxide coating of plagioclase and perthite, was also being released to solution (Table 3).

The isotopic ratios $^{206}Pb/^{207}Pb$ and $^{87}Sr/^{86}Sr$ record several stages during the mineral separate and whole rock dissolution experiments (Fig. 1a,b). The values of both ratios in the whole rock dissolution experiment fall within the range of values defined by the total digestion and the dissolution experiments of plagioclase, perthite, and biotite + chlorite (Fig. 1a,b). On the other hand, the behavior of $^{208}Pb/^{207}Pb$ in the whole rock dissolution experiment is much more erratic, and although the $^{208}Pb/^{207}Pb$ values in the whole rock dissolution experiment fall between the values of $^{208}Pb/^{207}Pb$ released by the dissolution of the plagioclase, perthite, and biotite + chlorite fractions, they all fall below the values of the total digested minerals (Fig. 1c). The drying of the whole rock sample after 1220 h caused substantial shifts in the values of $^{206}Pb/^{207}Pb$ and $^{87}Sr/^{86}Sr$ released to solution but not in $^{208}Pb/^{207}Pb$ (Fig. 1a,b,c).

4. DISCUSSION

4.1. Mass Balance Calculations on the Output Solutions

The major elemental composition of the output solutions of the minerals and the whole rock dissolution experiments (Table 3) were used to perform a mass balance calculation using the composition of the major minerals determined by electron microprobe as endmembers (Table 2). This calculation is based on the assumption that the minerals weather congruently, which indeed is the case most of the time. According to our calculations, plagioclase, K-feldspar, biotite, and chlorite dissolved congruently under far-from-equilibrium conditions, in the experiments with the bulk granite and with the plagioclase- and perthite-rich fractions. The solutions in all these experiments were undersaturated with respect to other primary and secondary minerals. In the absence of experimental data regarding the effect of deviation from equilibrium on the dissolution rate of accessory minerals, we can not verify that they all dissolved under far-from-equilibrium conditions. The dissolution of the biotite and chlorite in the biotite + chlorite–rich fraction (but not in the bulk granite) was noncongruent (Ganor et al., in press). In the first step, the concentration of Na in solution was attributed to the dissolution of plagioclase (assuming that the plagioclase An_{12-15} and albite within the perthite weather at a similar rate). Then the initial concentrations of Ca, Si, Al, and K were corrected based on their molar ratios to Na in plagioclase (Table 2). In the second step, all the Mg was attributed to the dissolution of biotite and chlorite (assuming equal rates of Mg release) and the concentrations of the other elements were corrected accordingly. In the third step, all the remaining K was attributed to the dissolution of the K-feldspar within the perthite. The remaining Ca was attributed to the dissolution of calcite and/or apatite. Because Ca, K, Na, and Mg were used for the calculations being the characteristic elements, their concentrations were 100% accounted for. Iron, Al, and Si were corrected accordingly, and with the exception of the first 2–3 samples, the calculations accounted for more than 90% of the Fe, whereas Si and Al were overconsumed by 13% and 25%, respectively. The change in the calculated proportions of the four major minerals (plagioclase, biotite + chlorite, K-feldspar, and calcite/apatite) with time during the experiments illustrates the dynamic nature of the weathering process and the strong effect of the stage (or degree) of weathering on the relative contribution of the different minerals on the release of elements from the rock (Fig. 2a–d). In the perthite-rich mineral separate, impurities of plagioclase and albite within the perthite dominate the composition of the output solution. In the whole rock dissolution experiment, calcite/apatite dissolution is dominant in the first 100 h, biotite is dominant after the initial 100 h, and after ~1000 h plagioclase dissolution is dominant (Fig. 2a–d).

Triangular diagrams of elemental composition of the whole rock output solutions (Fig. 3a: Mg-Ca-Na, and Fig. 3b: Mg-K-Na) provide additional insight into the dissolution behavior of these minerals. The compositions of the minerals biotite, chlorite, plagioclase, K-feldspar (the purest endmember that we could analyze within the perthite), and calcite are also plotted on the diagrams to indicate the stoichiometry of elemental release during the dissolution of each mineral. The first two output solution samples in the whole rock dissolution experiment (50 and 120 h) display a large contribution of Ca from calcite/apatite (Fig. 3a). All other samples plot much closer to the line connecting the biotite + chlorite and plagioclase endmembers, although they approach a more Na-rich plagioclase endmember than the one analyzed by the electron-probe, verifying that the plagioclase within the perthite is close in composition to pure albite. The second triangular diagram (Fig. 3b) reveals another interesting behavior of the dissolving minerals, which manifests itself in the behavior of K release. All of the output solutions (except the ones collected at the end of the experiment) plot in the triangle defined by chlorite, biotite, and plagioclase. The last few samples plot outside this triangle, possibly representing a growing influence of K-feldspar dissolution on the composition of the whole rock output solutions.

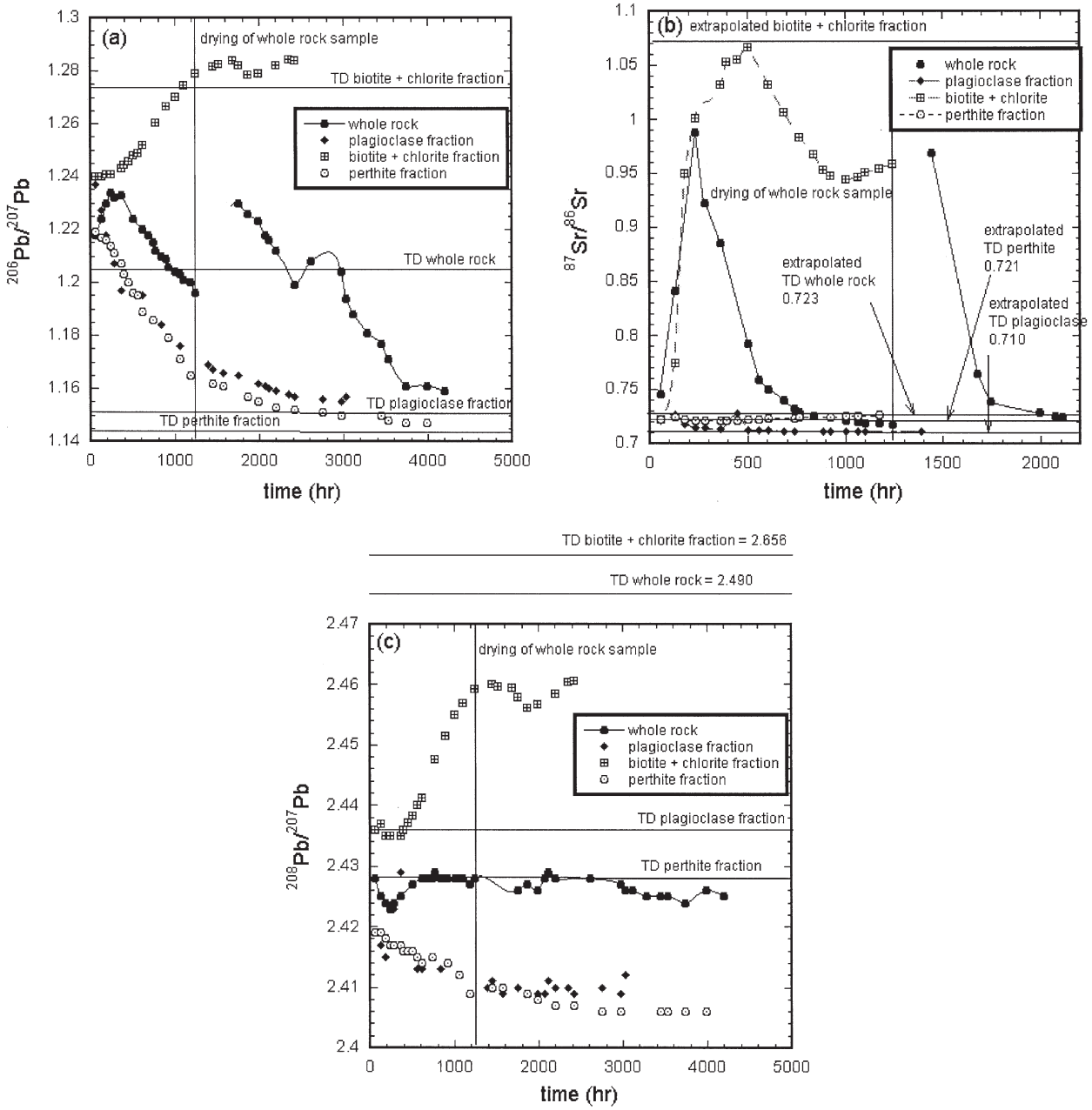

Fig. 1. (a) $^{206}Pb/^{207}Pb$ values of rock and mineral fractions released to solution as a function of time. The horizontal lines represent the values of the total digests of the whole rock and the mineral fractions. (b) $^{87}Sr/^{86}Sr$ values of rock and mineral fractions released to solution as a function of time. (c) $^{208}Pb/^{207}Pb$ values of rock and mineral fractions released to solution as a function of time.

4.2. Lead and Sr Isotopic Ratios in Whole Rock and Mineral Dissolution Experiments

Changes in the isotopic composition of Pb and Sr released by the dissolution of the whole rock sample reflect the release of these elements from the various minerals, which have contrasting isotopic ratios (Tables 1 and 2). Indeed, the $^{206}Pb/^{207}Pb$, $^{208}Pb/^{207}Pb$, and $^{87}Sr/^{86}Sr$ values of the whole rock dissolution experiment fall between the values of Pb and Sr released from the plagioclase-rich, perthite-rich, and biotite + chlorite–rich fractions (Fig. 1a,b,c). The $^{206}Pb/^{207}Pb$ and $^{87}Sr/^{86}Sr$ ratios released by the dissolution of the whole rock are bracketed by the ratios of the total digest of the mineral-separates (Fig. 1a,b). On the other hand, the $^{208}Pb/^{207}Pb$ values of the whole rock dissolution samples fall below the values for digests of each of these mineral fractions (Fig. 1c). This suggests that a significant fraction of the thorogenic accessory minerals are less susceptible to dissolution and hence do not release their ^{208}Pb-enriched Pb.

A hypothetical whole rock composition was calculated from

Table 3. Concentrations (μM) of major and minor elements and isotopic ratios of Pb and Sr in the output solutions. All solutions were at 25°C ± 0.5, and pH = 1.0–1.1.

a) Whole rock experiment

	time (h)	V (mL)	Si	Al	Ti	Na	Ca	K	Fe	Mg	Pb	Sr	$^{206}Pb/^{207}Pb$	$^{208}Pb/^{207}Pb$	$^{87}Sr/^{86}Sr$
WR-B-1	51	46	309	377	6	119	440	117	354	100	1.9E−02	4.7E−01	1.218	2.428	0.74597
WR-B-2	99	46	443	470	14	51	131	144	462	129	7.8E−03	1.6E−01	1.224	2.425	0.84114
WR-B-3	171	69	465	398	18	36	41	127	432	120	4.6E−03	6.1E−02	1.230	2.424	
WR-B-4	219	47	479	357	22	33	27	95	389	110	2.1E−03	4.9E−02	1.234	2.423	0.98772
WR-B-5	263	43	497	349	25	40	27	79	377	106	1.6E−03	5.3E−02	1.232	2.424	0.92271
WR-B-6	386	52									3.3E−03	9.3E−02	1.233	2.425	0.88528
WR-B-8	507	73	470	294	20	38	28	39	337	87	3.0E−02	6.0E−02	1.224	2.427	0.79179
WR-B-9	559	49	471	298	17	43	30	30	333	87	2.9E−02	6.6E−02			0.75852
WR-B-10	604	43	453	288	15	44	29	28	316	84	2.8E−02		1.220	2.428	0.75031
WR-B-11	682	46	436	273	13	46	29	25	294	78	2.6E−02	7.6E−02	1.218	2.428	0.74027
WR-B-12	739	55	461	271	11	51	28	21	295	75	2.4E−02		1.215	2.428	0.73216
WR-B-13	770	30	453	274	11	54	29	20	282	74	2.3E−02	8.5E−02	1.212	2.429	0.72863
WR-B-14	838	67	450	264	10	55	28	17	272	69	2.1E−02		1.210	2.428	0.72565
WR-B-15	892	53	445	261	9	64	27	18	253	66	1.8E−02	8.6E−02	1.209	2.428	
WR-B-16	939	48	454	259	9	74	26	22	245	63	1.7E−02		1.206	2.428	
WR-B-17	1008	70	432	240	8	81	24	20	221	56	1.5E−02	9.0E−02	1.204	2.428	0.72102
WR-B-18	1052	44	448	244	8	71	24	17	212	55	1.4E−02		1.203	2.428	0.72038
WR-B-19	1101	49	473	253	8	76	25	18	214	55	1.4E−02	1.0E−01	1.201	2.428	0.71938
WR-B-20	1173	71	484	252	7	79	25	21	206	53	1.3E−02		1.200	2.427	0.71848
WR-B-21	1221	50	484	247	7	82	24	18	191	48	1.1E−02	1.0E−01	1.196	2.428	0.71792
WR-B-26	1438	62	412	273	25	24	19	62	306	79	1.1E−02	4.3E−02	1.230	2.426	0.96918
WR-B-29	1678	90	322	198	11	25	19	22	230	60	1.1E−01	4.3E−02	1.226	2.427	0.76490
WR-B-31	1782	67	317	207	9	30	19	16	233	62			1.223	2.426	0.73940
WR-B-33	1894	59	335	201	8	34	18	12	218	57	2.5E−02	5.3E−02	1.218	2.428	
WR-B-34	2012	141	324	186	7	40	17	18	204	51	2.1E−02		1.216	2.429	0.72868
WR-B-35	2060	61	351	203	7	62	19	15	221	53	1.7E−02		1.212	2.428	0.72599
WR-B-36	2108	61	349	195	7	47	18	14	177	50			1.199	2.390	0.72447
WR-B-38	2229	58	356	192	6	51	18	12	161	45		3.4E−02	1.208	2.428	
WR-B-41	2396	57	460	209	6	67	19	15	151	42			1.204	2.427	
WR-B-45	2611	58	506	212	5	85	19	20	117	31	5.6E−03		1.194	2.426	0.71851
WR-B-47	2735	56	562	219	4	100	19	18	96	27	9.5E−03		1.188	2.426	
WR-B-51	2949	59	488	201	3	102	17	20	59	16			1.181	2.425	
WR-B-52	3021	93	523	207	3	106	16	23	55	15					
WR-B-54	3115	60	562	222	2	119	17	23	47	13			1.177	2.425	
WR-B-57	3284	57	588	232	2	139	17	24	32	6			1.171	2.425	0.71563
WR-B-60	3452	58	709	258	1	174	17	26	25	2					
WR-B-61	3525	94	671	259	0	171	17	28	11	3					
WR-B-64	3694	94	752	271	1	177	18	32	16	1			1.161	2.424	0.71567
WR-B-70	4031	95	696	262	0	176	16	29	8	1			1.161	2.426	0.71576
WR-B-73	4197	90	660	250	0	169	15	33	6	1			1.159	2.425	0.71607

the mineral separate digests using their isotopic values, elemental concentrations, and distribution in the rock (Table 1). As indicated previously, plagioclase, perthite, and biotite + chlorite contain most of the major cations (and Pb and Sr) in the rock (Table 1) and weather substantially faster than quartz (White and Brantley, 1995), hence, they control the release of these elements during the dissolution of the rock and were used for the hypothetical rock calculations. The major elements, Sr, U, and Pb concentrations yield similar values in the hypothetical rock and in the measured whole rock digests (Table 1). The Th content, however, is four times lower in the hypothetical rock than in the measured whole rock digest. This suggests that in addition to having low susceptibility to dissolution, a significant fraction of the thorogenic accessory mineral fraction was lost during the process of mineral separation, which excluded the heaviest mineral fraction. The fact that the hypothetical $^{206}Pb/^{207}Pb$ and $^{208}Pb/^{207}Pb$ values (1.15 and 2.45) are significantly lower than the actual whole rock values (1.21 and 2.49) further demonstrates the importance of these lost accessory phases in controlling the isotopic composition of Pb in the rock.

Based on the $^{206}Pb/^{207}Pb$ values of the rock sample, four stages of rock dissolution can be defined (Fig. 1a): (1) an initial stage (first 200 h) with an increase in $^{206}Pb/^{207}Pb$ values towards relatively radiogenic values. This increase reflects a transition from the beginning of the experiments, in which the isotopic signal is dominated by dissolution of traces of nonradiogenic minerals, to the next stage, in which the isotopic signal is dominated by dissolution of more radiogenic minerals. (2) A second stage of constant and radiogenic $^{206}Pb/^{207}Pb$ values (200–400 h). (3) A decrease in the $^{206}Pb/^{207}Pb$ values (400–1000 h) when $^{206}Pb/^{207}Pb$ values in solution are higher than whole rock digest values. (4) A final stage (1000 h to the end of the experiment) when $^{206}Pb/^{207}Pb$ values in solution are lower than whole rock digest values.

In general, $^{87}Sr/^{86}Sr$ values reveal a similar story to $^{206}Pb/^{207}Pb$. The major difference is that the initial stage of high $^{87}Sr/^{86}Sr$ is shorter than for $^{206}Pb/^{207}Pb$, and the decrease in $^{87}Sr/^{86}Sr$ values starts after only 150 h rather than after 400 h (Fig. 1a,b). The same observation holds for the impact of the whole rock drying, which shifts both isotopic ratios substan-

Table 3. (Continued)

b) K-feldspar experiment (Mg and Ti were below detection limit)

	time (h)	V (mL)	Si	Al	Ti	Na	Ca	K	Fe	Mg	Pb	Sr	$^{206}Pb/^{207}Pb$	$^{208}Pb/^{207}Pb$	$^{87}Sr/^{86}Sr$
K-Feld-B-1	71	70	107	101		43	94	46	21	0	6.5E−02	1.4E−01	1.219	2.419	0.72216
K-Feld-B-2	123	53	139	72		19	38	25	13	0	4.4E−02	7.7E−02	1.217	2.419	0.72429
K-Feld-B-3	171	50	164	77		20	32	26	10	0	4.5E−02	8.2E−02	1.216	2.418	0.72215
K-Feld-B-4	236	67	174	76		16	27	26	8	0	4.1E−02	8.3E−02	1.214	2.417	0.72083
K-Feld-B-5	284	49	226	98		28	29	29	9	0	4.6E−02	1.1E−01	1.211	2.417	0.72067
K-Feld-B-6	332	50	274	119		53	31	38	11	0	1.1E−01		1.207	2.417	0.72080
K-Feld-B-7	407	84	313	134		51	29	43	13	0	3.9E−02	1.3E−01	1.203	2.416	0.72116
K-Feld-B-8	452	46	372	155		60	29	47	14	0	3.6E−02		1.200	2.416	0.72157
K-Feld-B-9	498	47	388	161		66	28	48	14	0	3.4E−02	1.3E−01	1.196	2.416	0.72195
K-Feld-B-10	573	77	405	162		70	26	50	13	0	3.1E−02		1.195	2.415	0.72231
K-Feld-B-11	623	52	475	173		74	24	51	13	0	2.6E−02	1.5E−01	1.189	2.414	0.72289
K-Feld-B-12	666	43												0.72310	
K-Feld-B-13	741	76	527	191		86	22	56	12	0	2.5E−02		1.186	2.415	0.72340
K-Feld-B-14	789	49													0.72398
K-Feld-B-16	910	77	599	206		95	19	59	9	0	1.8E−02	1.6E−01	1.179	2.414	0.72471
K-Feld-B-17	957	47													0.72515
K-Feld-B-19	1075	70	654	234		111	18	69	7	0	1.6E−02	1.7E−01	1.171	2.412	0.72555
K-Feld-B-21	1177	53	677	249		117	18	74	6	0	1.4E−02		1.165	2.409	0.72621
K-Feld-B-24	1414	65									3.8E−02				
K-Feld-B-25	1459	46	608	204		107	12	58	3	0	5.1E−03	7.1E−02	1.162	2.410	
K-Feld-B-27	1583	67	673	229		116	12	67	2	0	1.1E−02	1.7E−01	1.161	2.410	
K-Feld-B-31	1844	50	711	258		131	12	73	2	0	9.4E−03		1.157	2.409	
K-Feld-B-33	1964	45	749	260		136	11	74	2	0	9.1E−03		1.155	2.408	
K-Feld-B-35	2087	78									8.2E−03				
K-Feld-B-37	2180	50											1.153	2.407	
K-Feld-B-40	2426	81	946	320		167	11	94	1	0			1.152	2.407	
K-Feld-B-46	2757	75	969	333		173	10	92	1	0			1.151	2.406	
K-Feld-B-50	2975	50											1.150	2.406	
K-Feld-B-55	3261	74	1084	357		192	11	106	0	0					
K-Feld-B-58	3429	76	1082	339		179	9	97	1	0			1.150	2.406	
K-Feld-B-61	3602	78	1066	343		179	9	101	0	0			1.148	2.406	
K-Feld-B-64	3767	75	1073	353		183	9	105	0	0			1.147	2.406	
K-Feld-B-67	3933	72	1065	366		189	9	110	1	0			1.147	2.406	

tially towards radiogenic (i.e., higher) values, but with a much more rapid subsequent decrease in the $^{87}Sr/^{86}Sr$ values (Fig. 1a,b). Another difference between the Pb and Sr isotopic ratios is the behavior of the less-radiogenic plagioclase and perthite mineral separates. Whereas $^{87}Sr/^{86}Sr$ values released by the dissolution of these minerals remain almost constant and are very similar to their total digest values, the $^{206}Pb/^{207}Pb$ values of these minerals initially released to solution are substantially more radiogenic than their total digest values, possibly reflecting the release of more radiogenic Pb from the Fe-oxide coatings on plagioclase and perthite (Fig. 1a,b). This suggestion is supported by the observation that the concentrations of Fe and $^{206}Pb/^{207}Pb$ values in the output solutions of plagioclase and perthite mineral separates co-vary, and after more than 3000 h when $^{206}Pb/^{207}Pb$ ratio approaches the nonradiogenic values of the total digested minerals, Fe concentrations are the lowest (Table 3).

The values of $^{87}Sr/^{86}Sr$ released by biotite initially reach exceptionally radiogenic values, probably because of preferential release of ^{87}Sr (and K) from the interlayer sites. After this stage, there is a slower release of Sr from the octahedral sites of biotite (Blum and Erel, 1997; Taylor et al., 2000a,b). This again suggests that whereas the Pb isotopic composition is controlled mostly by a balance between the dissolution of accessory phases and that of the major minerals, changes in Sr isotopes are also influenced by the release of Sr from interlayer sites of biotite (Blum and Erel, 1997; Harlavan and Erel, 2002).

4.3. Lead and Strontium Isotopes Combined With Major Elements

To gain more insight into the behavior of $^{206}Pb/^{207}Pb$, $^{208}Pb/^{207}Pb$, and $^{87}Sr/^{86}Sr$ ratios during mineral dissolution, we calculated the isotopic composition in the dissolution of the hypothetical rock composed of plagioclase, K-feldspar, biotite + chlorite, and calcite/apatite. This was done using the calculated proportion of the minerals in the whole rock output solutions based on the major element content of the solution (Fig. 2d). The values in Figure 2d were then multiplied by the Pb or Sr concentration and the isotopic composition of Pb or Sr in these phases (Table 2b). The concentrations of Pb and Sr in each pure phase (except Pb in biotite + chlorite) were assumed to be equal to their concentrations in the mineral separates (Tables 1 and 2). The concentration of Pb in the biotite + chlorite pure minerals was assumed to be lower than in the biotite + chlorite mineral separate, because biotite + chlorite contains a large amount of Pb-rich inclusions, some of which are considerably more resistant to weathering than biotite (Table 2). The actual value assigned for Pb concentration in the biotite (10 vs. 35 ppm) was the fitting parameter in the calcu-

Table 3. (Continued)

c) Plagioclase experiment (Mg and Ti were below detection limit)

	time (h)	V (mL)	Si	Al	Ti	Na	Ca	K	Fe	Mg	Pb	Sr	$^{206}Pb/^{207}Pb$	$^{208}Pb/^{207}Pb$	$^{87}Sr/^{86}Sr$
pl-B-1	49	40	269	274		281	272	74	66	36	1.4E−01	3.6E−01	1.237	2.419	0.72081
pl-B-2	118	65	307	189		106	66	39	54	20	7.7E−02	1.6E−01	1.227	2.417	0.72630
pl-B-3	169	47	351	180		106	51	23	38	0	5.9E−02	1.7E−01	1.218	2.415	0.71763
pl-B-4	220	48	384	190		115	49	22	35	0	5.4E−02	1.8E−01	1.213	2.417	0.71497
pl-B-5	290	66	414	198		121	45	19	33	0	4.8E−02	2.0E−01	1.207	2.423	0.71403
pl-B-6	387	83	484	224		148	45	24	36	0	2.6E−02	2.4E−01	1.197	2.429	0.71302
pl-B-7	457	71	679	246		138	14	69	4	0	4.5E−02				0.72788
pl-B-8	503	43	477	211		147	34	20	29	0	1.1E−02				0.71231
pl-B-9	561	55	533	229		168	35	22	30	0	2.5E−02	2.2E−01	1.195	2.413	0.71206
pl-B-10	623	59	574	248		177	34	19	29	0	2.2E−02	2.2E−01	1.195	2.413	0.71187
pl-B-11															0.71161
pl-B-12	793	112									1.6E−02				0.71140
pl-B-13	839	44	716	299		215	34	23	26	0	1.6E−02	2.4E−01	1.184	2.413	
pl-B-14	887	45									1.6E−02				0.71125
pl-B-15															0.71106
pl-B-16	1007	43									1.3E−02				0.71096
pl-B-17	1055	45	728	296		221	29	24	17	0	1.1E−02		1.176	2.412	0.71092
pl-B-18	1130	71									1.0E−02				0.71084
pl-B-20	1390	43	1096	410		308	35	28	13	0			1.169	2.410	0.71074
pl-B-22	1514	42	1121	411		321	34	31	10	0			1.167	2.411	
pl-B-23	1558	42	1169	433		332	35	32	10	0			1.166	2.409	
pl-B-26	1728	44	1078	382		296	30	27	7	0			1.165	2.410	
pl-B-30	1969	74	1127	405		316	29	29	4	0			1.162	2.409	
pl-B-32	2063	44	1152	411		328	29	32	4	0			1.161	2.409	
pl-B-37	2353	42											1.160	2.411	
pl-B-38	2399	39											1.159	2.410	
pl-B-39	2473	74	1241	479		351	31	30	11	0			1.158	2.410	
pl-B-40	2520												1.157	2.409	
pl-B-42	2645	76	1246	485		345	30	29	14	0					
pl-B-45	2810	74											1.156	2.410	
pl-B-48	2976	59	1258	487		343	30	31	13	0			1.155	2.409	
pl-B-49	3023	56	1211	475		333	31	33	13	0			1.157	2.412	

lations. The isotopic compositions of Sr and Pb in the pure minerals were obtained from the dissolution experiments of the mineral separates, assuming that when the pure phases were contributing the highest proportions of elements to solution (Fig. 2a,b,c) the isotopic compositions of the solutions (Fig. 1a,b,c) were good approximations of the compositions of the pure minerals. The calcite/apatite phase had a significant contribution to the whole rock dissolution only in the first ~150 h of the dissolution experiment, and because the $^{206}Pb/^{207}Pb$ and $^{87}Sr/^{86}Sr$ values of the output solutions were low during this period (Fig. 1a,b), it is reasonable to assume that the contribution at that stage was mostly from calcite, as a high proportion of apatite should have had elevated the $^{206}Pb/^{207}Pb$ values (Chen and Moore, 1982; Chen and Tilton, 1991; James, 1992; Mattinson, 1978). On the other hand, after ~1000 h apatite and not calcite was the main mineral inclusion controlling the release of Pb from the biotite + chlorite–rich phase. This is evident from both the excess of Ca (Fig. 2b) and the radiogenic Pb values (Fig. 1a,c). Namely, at that stage the released Pb was more radiogenic (Fig. 1a,c; $^{206}Pb/^{207}Pb = 1.285$; $^{208}Pb/^{207}Pb = 2.46$) than Pb released from the biotite + chlorite–rich phase after ~ 350 h, when the proportion of biotite + chlorite pure minerals in the biotite + chlorite–rich mineral separate was the highest (Fig. 2b; Fig. 1a,c; $^{206}Pb/^{207}Pb = 1.242$; $^{208}Pb/^{207}Pb = 2.435$). Because calcite/apatite phase has the strongest impact on the composition of the whole rock dissolution products in the initial phases of dissolution (less than 150 h; Fig. 2d), we use calcite and not apatite values for the calculation of the isotopic composition of Pb and Sr released from the hypothetical rock. The values used for Sr and Pb concentrations and isotopic compositions in calcite in Table 2b are assumed to be similar to plagioclase, the other Ca-rich mineral.

The isotopic composition of Pb and Sr that would be released by the hypothetical rock is plotted against the measured values from the rock dissolution experiments (Fig. 4a,b,c). The hypothetical rock is composed of the three major minerals and calcite. An agreement between the measured isotopic composition and the calculated dissolution of the hypothetical rock would indicate that the change with time in the isotopic composition during the dissolution of the granite is only due to changes in the relative contribution of the four phases. $^{206}Pb/^{207}Pb$ values of the hypothetical rock (Fig. 4a) form two distinctive groups. The first group of samples plot along the 1:1 line and are solutions released during the period of dominance of biotite + chlorite and plagioclase on the dissolution process (150–2600 h).

The second group of samples plot below the 1:1 line and are from the early stage of dissolution (first 120 h) and the last stage of dissolution (2600–4200 h). During these stages, the actual values of $^{206}Pb/^{207}Pb$ are higher than the calculated ones, probably because the release of Pb is affected by the dissolution of radiogenic accessory phases that are not accounted for in the calculations. Generally, in all phases of the dissolution experiment $^{206}Pb/^{207}Pb$ values trace the proportion of the major

Table 3. (Continued)

d) Biotite + chlorite experiment

	time (h)	V (mL)	Si	Al	Ti	Na	Ca	K	Fe	Mg	Pb	Sr	$^{206}Pb/^{207}Pb$	$^{205}Pb/^{207}Pb$	$^{87}Sr/^{86}Sr$
Mag-B-1	43	32	888	866	3	1935	1738	139	963	652	9.3E−01	1.7E+00	1.240	2.436	0.72270
Mag-B-2	163	102	1380	1270	6	454	598	239	1125	929	1.2E+00	1.0E+00	1.240	2.437	0.77500
Mag-B-3	209	39	1615	1380	13	68	109	274	1261	1066	4.5E−01	2.1E−01	1.241	2.435	0.94976
Mag-B-4	257	41	1726	1412	20	37	78	257	1288	1114	3.0E−01	1.6E−01	1.241	2.435	1.00126
Mag-B-5	329	62	1745	1380	32	23	73	232	1265	1073	2.4E−01	1.3E−01	1.243	2.435	1.03211
Mag-B-6	378	41	1896	1458	47	23	91	234	1356	1142	2.0E−01	1.2E−01	1.244	2.436	1.05351
Mag-B-7	425	40	1825	1382	58	20	94	212	1302	1072	1.7E−01	1.0E−01	1.246	2.437	1.05609
Mag-B-8	500	64	1806	1349	70	20	103	198	1294	1024	1.8E−01	1.1E−01	1.248	2.438	1.06657
Mag-B-9	546	38	2121	1579	93	23	143	218	1507	1190	1.3E−01		1.249	2.440	
Mag-B-10	594	41	1932	1439	101	22	143	191	1397	1089	1.2E−01		1.252	2.441	1.03243
Mag-B-11	714	104									1.2E−01				1.00693
Mag-B-12	761	39	2381	1701	152	15	227	180	1659	1245	1.2E−01		1.260	2.448	0.98374
Mag-B-13	839	67									1.1E−01				0.96801
Mag-B-14	884	38	2657	1895	190	13	282	173	1860	1359	1.2E−01		1.267	2.452	0.95285
Mag-B-15	928	38									1.1E−01				0.94743
Mag-B-16	1001	62	2356	1633	190	13	269	149	1640	1165	1.1E−01		1.270	2.455	0.94404
Mag-B-17	1052	43									1.1E−01				0.94656
Mag-B-18	1098	40	2292	1614	186	10	262	142	1641	1122	9.0E−02		1.274	2.457	0.95065
Mag-B-19	1170	62									9.7E−02				0.95431
Mag-B-20	1217	40									9.0E−02				0.96207
Mag-B-21	1265	41	2277	1580	188	10	257	135	1638	1064	8.3E−02		1.279	2.459	0.95879
Mag-B-24	1434	38	2323	1606	189	11	254	124	1684	1073			1.282	2.460	
Mag-B-25	1507	64	2291	1583	188	13	250	125	1669	1050			1.283	2.460	
Mag-B-28	1675	59	2936	2197	234	19	369	228	2380	1369			1.284	2.460	
Mag-B-29	1723	48	2773	2069	202	26	227	247	2361	1230			1.282	2.458	
Mag-B-31	1843	65	2955	2231	195	17	222	255	2442	1323			1.279	2.456	
Mag-B-34	2016	66	2907	2064	190	20	212	198	2236	1234			1.279	2.457	
Mag-B-37	2180	63	2627	1810	181	21	198	162	1986	1089			1.282	2.459	
Mag-B-40	2346	61	2123	1441	159	21	182	123	1526	885			1.285	2.460	
Mag-B-41	2393	40	2161	1467	157	20	186	116	1585	908			1.284	2.461	
Mag-B-43	2445												1.288	2.461	
Mag-B-46	2614												1.288	2.461	

minerals in the output solutions, and provide a good proxy for the dissolution of the studied granitoid rock. This assertion is supported by the observation that $^{206}Pb/^{207}Pb$ values correspond systematically to changes in ([Na]+[Ca])/[Mg] values (Fig. 5a). The ([Na]+[Ca])/[Mg] ratio largely represents the proportions of plagioclase vs. biotite + chlorite in the output solutions of the whole rock. In the course of the experiment they shift from low ([Na]+[Ca])/[Mg] and high $^{206}Pb/^{207}Pb$ values, when biotite + chlorite dominates the solution composition, to high ([Na]+[Ca])/[Mg] and low $^{206}Pb/^{207}Pb$ values, when plagioclase dominates the solution composition (Fig. 5a).

In contrast to $^{206}Pb/^{207}Pb$, the values of both $^{87}Sr/^{86}Sr$ and $^{208}Pb/^{207}Pb$ calculated for the release by the hypothetical rock are different than the values of $^{87}Sr/^{86}Sr$ and $^{208}Pb/^{207}Pb$ actually released by the whole rock dissolution experiment (Fig. 4b,c). As suggested earlier, $^{87}Sr/^{86}Sr$ values released by the rock dissolution process reflect mostly the depletion of interlayer sites in biotite and the dissolution of calcite in the early stages of rock dissolution. It was proposed in a previous study (White et al., 1999) that Sr release to solution from biotite is not congruent with K, either due to the extreme sensitivity of Sr isotope ratios to the dissolution of trace Ca-bearing phases with low $^{87}Sr/^{86}Sr$, and/or the preferential retention of Sr relative to K in biotite. A plot of $^{87}Sr/^{86}Sr$ vs. K for our whole rock output solutions supports this idea (Fig. 5b). The initial values of Sr are much less radiogenic than expected from K concentrations due to the impact of trace calcite. With the progress of the dissolution experiment there is a better correlation between K and Sr isotopic values, reflecting the impact of octahedral sites in biotite and of plagioclase (with low K and $^{87}Sr/^{86}Sr$ values) on the dissolution solutions. Hence, $^{87}Sr/^{86}Sr$ released by biotite changes with time; initially it reaches exceptionally radiogenic (i.e., high) values, and later, when Sr is released from the octahedral sites of biotite, it becomes much less radiogenic (Blum and Erel, 1997; Taylor et al., 2000a,b). Therefore, the values of $^{87}Sr/^{86}Sr$ released by our hypothetical rock reflect (and can be used to recognize) an important stage in which biotite interlayer sites are being depleted, a process that takes place during the initial phases of rock dissolution.

$^{208}Pb/^{207}Pb$ values of the hypothetical rock also do not resemble the actual measured $^{208}Pb/^{207}Pb$ values of the rock dissolution experiment (Fig. 4c). As shown earlier, the thorogenic minerals are not releasing their Pb in proportion to their host minerals and therefore the $^{208}Pb/^{207}Pb$ value of the output solution has a narrow range throughout the experiment (Fig. 1c, 4c). The lack of systematic behavior of $^{208}Pb/^{207}Pb$ vs. time in this study is very different from the one reported for natural soils and leaching experiments on granitoid rocks from the Wind River Mountains (Harlavan et al., 1998; Harlavan and Erel, 2002). In rocks from the Wind River Mountains, thorogenic minerals were among the first minerals to release their Pb and hence affected the $^{208}Pb/^{207}Pb$ values of the dissolution process. Thus, we caution that the Pb isotopes of weathering products strongly reflect

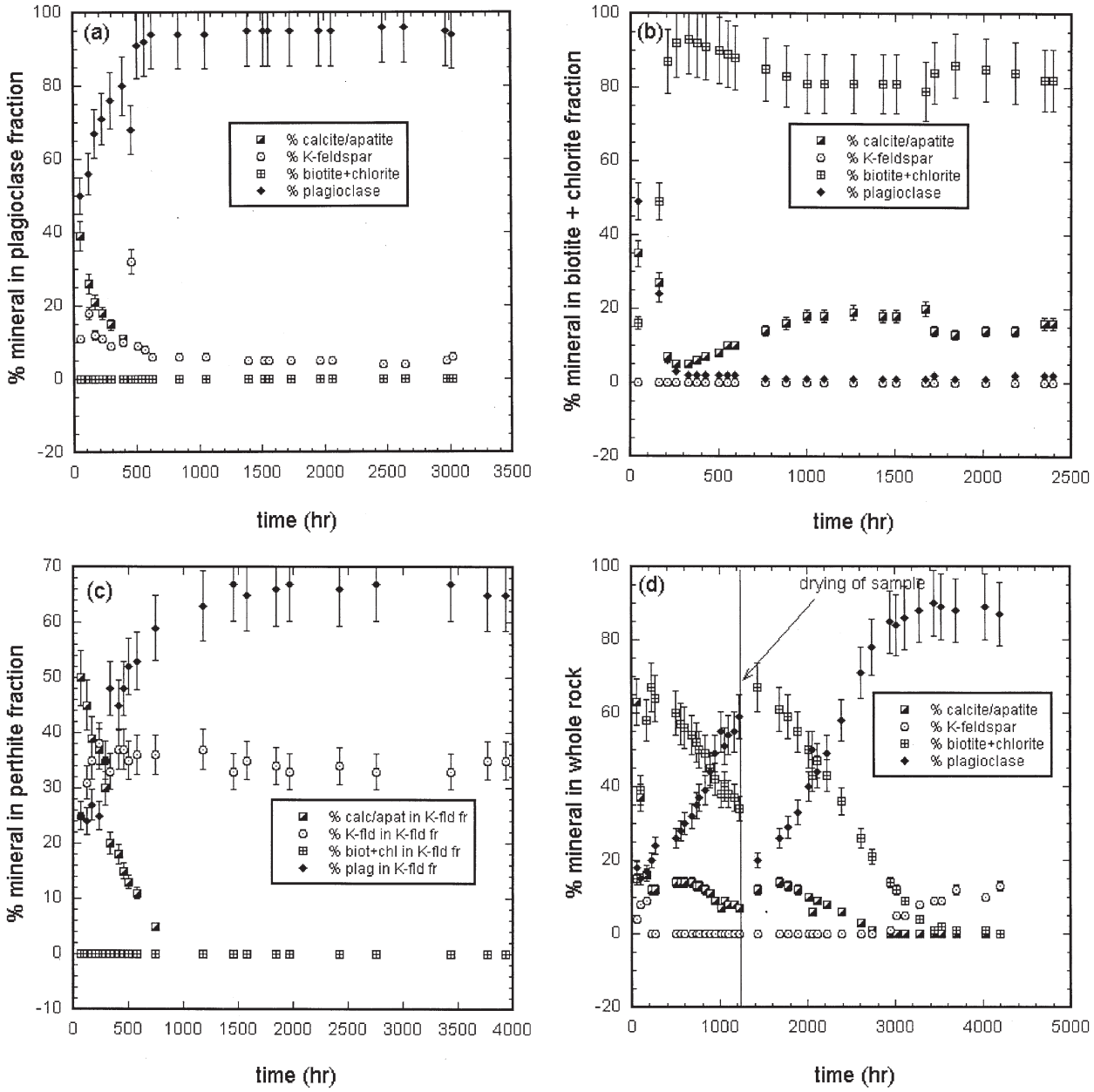

Fig. 2. Calculated (see text for details) proportions of plagioclase, biotite + chlorite, K-feldspar (within the perthite), and calcite/apatite in the output solutions as a function of time. Errors are dominated by uncertainties in the composition of the pure minerals. (a) Plagioclase-rich mineral separate. (b) Biotite + chlorite–rich mineral separate. (c) Perthite-rich mineral separate. (d) Whole-rock sample. The elevated contribution of K-feldspar in the initial stages of rock dissolution is most likely an artifact caused by excess K release from the interlayer of biotite.

the specific mineralogy of the dissolving rock and in particular the distribution and the nature of the accessory phases and their susceptibility to weathering.

The drying of the whole rock sample after 1220 h of the dissolution experiment caused a systematic effect where all the parameters except for $^{208}Pb/^{207}Pb$ shifted towards the biotite + chlorite value (Figs. 2d, 1a,b,c, Table 3). We attribute these shifts to changes in the characteristics of biotite (and/or chlorite), which accelerated the release of interlayer ions. To propose a more specific mechanism, additional experiments need to be done. Nevertheless, drying periods during the process of rock weathering should be ubiquitous in arid and semiarid environments, and might influence the weathering mechanism in various ways. Hence, drying/wetting should have far-reaching implications for interpretation of the climatic influence on rock weathering (White and Blum, 1995; White et al., 1999; Jacobson et al., 2002).

In summary, the isotopic compositions of Pb and Sr respond to several processes during the dissolution of granitoids. Changes in the values of $^{206}Pb/^{207}Pb$ reflect the dissolution of accessory phases included in major minerals, and changes in the values of $^{87}Sr/^{86}Sr$ reflect the release of

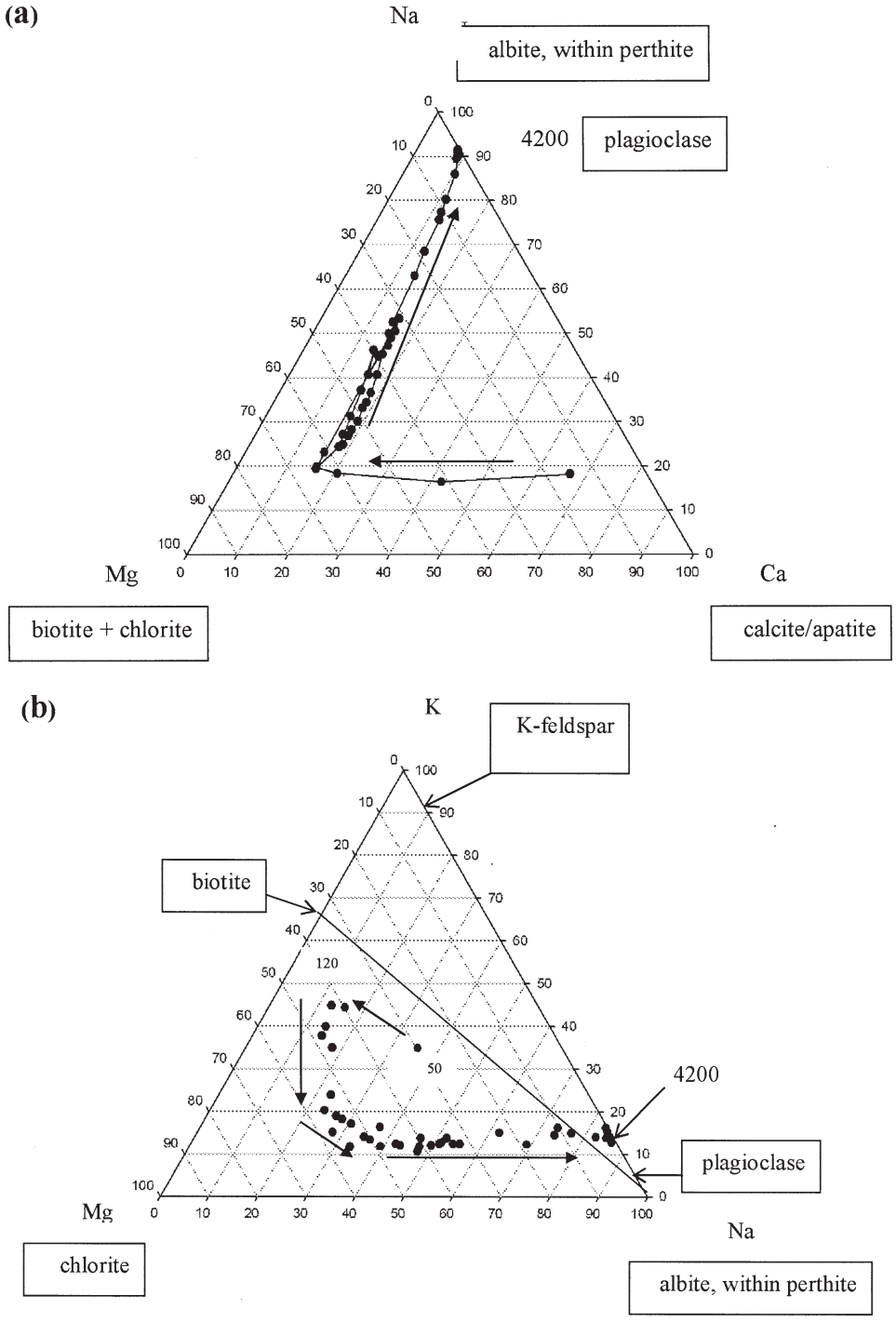

Fig. 3. (a) Molar Na-Ca-Mg triangular diagram of the solution released during the whole rock dissolution experiment. (b) Molar K-Mg-Na triangular diagram of the solution released during the whole rock dissolution experiment. Numbers indicate experimental duration in hours. Mineral compositions from electron microprobe analyses are also plotted on each diagram.

elements from interlayer sites in biotite and from traces of calcite/apatite. Comparing the shifts in isotope ratios with characteristic major element concentrations and ratios enables us to gain insight into the changing proportions of major rock-forming minerals in the output solutions. According to our experiments at pH 1 the initial stage of granitoid dissolution (<200 h of leaching) is controlled by the release of elements from traces of calcite and to a lesser extent from the interlayer sites in biotite. In the second stage of dissolution (200–400 h), biotite dissolution (mostly interlayer sites) controls the release of major and trace elements. In the third stage of dissolution (400–1000 h), bi-

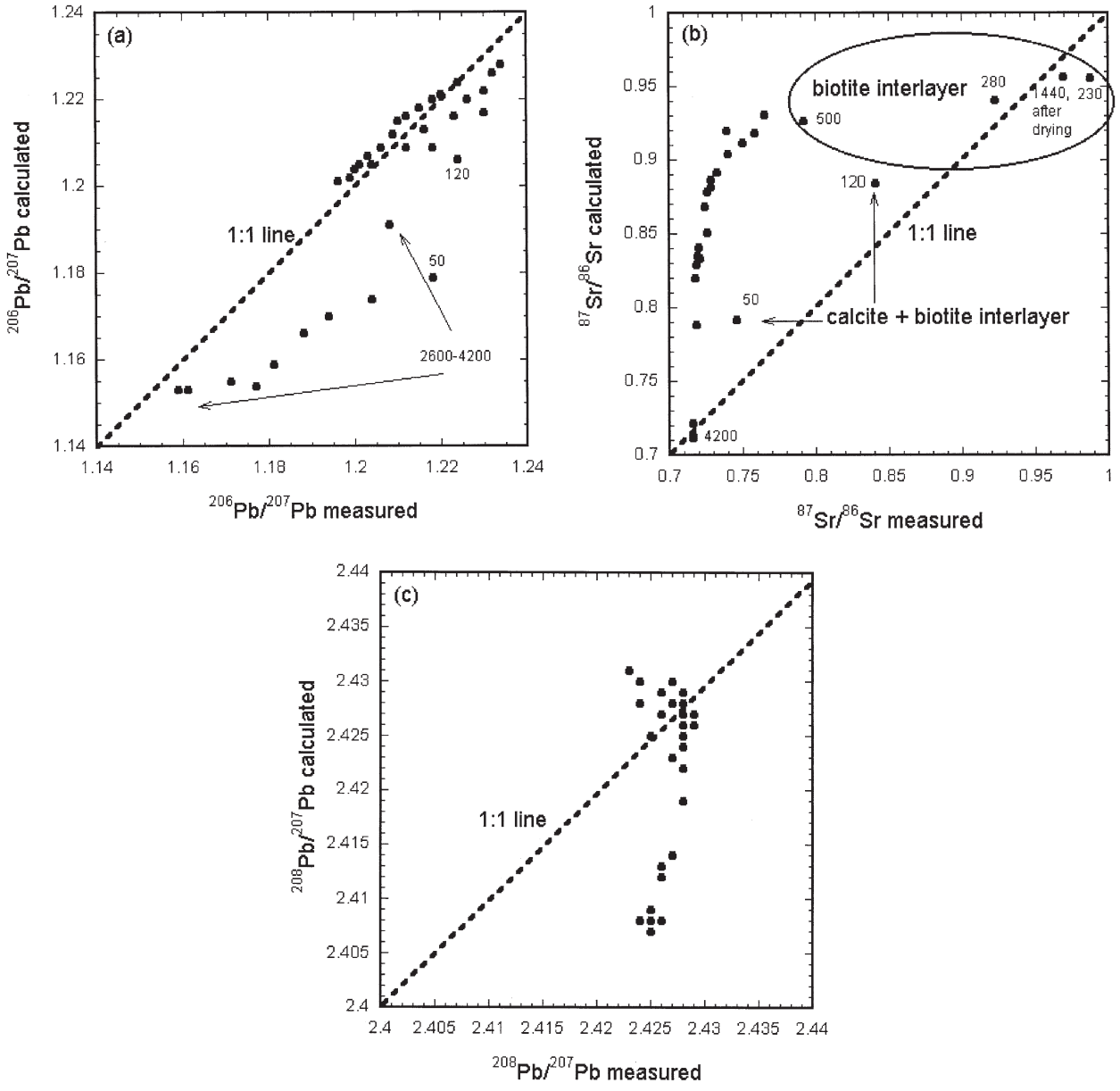

Fig. 4. Hypothetical rock (see text) vs. measured rock values released to solution during the dissolution experiments (a) $^{206}Pb/^{207}Pb$ (numbers indicate time [hours] from the beginning of the experiment); (b) $^{87}Sr/^{86}Sr$; (c) $^{208}Pb/^{207}Pb$.

otite, and to a lesser extent plagioclase, determines the elemental and isotopic compositions of the solution. In the fourth stage (>1000 h), plagioclase, and to a lesser extent biotite, influences the composition of elements released to solution. Although we observe systematic patterns in our experiments, to utilize this approach in natural systems, we need to compare the results of our dissolution experiments carried out at pH 1 and far from equilibrium, to conditions that prevail in natural weathering systems.

4.4. Low-pH Dissolution Experiments vs. Weathering Under Natural Conditions

The degree to which low-pH dissolution experiments can be used to understand natural weathering processes is a major issue in weathering studies (White and Brantley, 1995; White et al., 1999; White and Brantley, 2003). To address this question, we compare our experimental results for Pb and Sr isotope release with field measurements conducted by us in previous studies of granitoid soil chronosequences developed on glacial moraines in the Wind River Mountains, Wyoming and the Sierra Nevada, California, which have soil pH values in the range of 5–7 (Sorenson, 1986; Erel et al., 1994; Blum and Erel, 1995, 1997; Harlavan et al., 1998). In soils from the Wind River Mountains we observed that the isotopic composition of Sr in the labile fraction of the soil (defined as the ammonium acetate exchange fraction) decreased sharply with soil age from 400-year-old soils to 10,000- to 20,000-year-old soils (Blum and Erel, 1997). Lead isotopes in the labile fraction (weak-acid

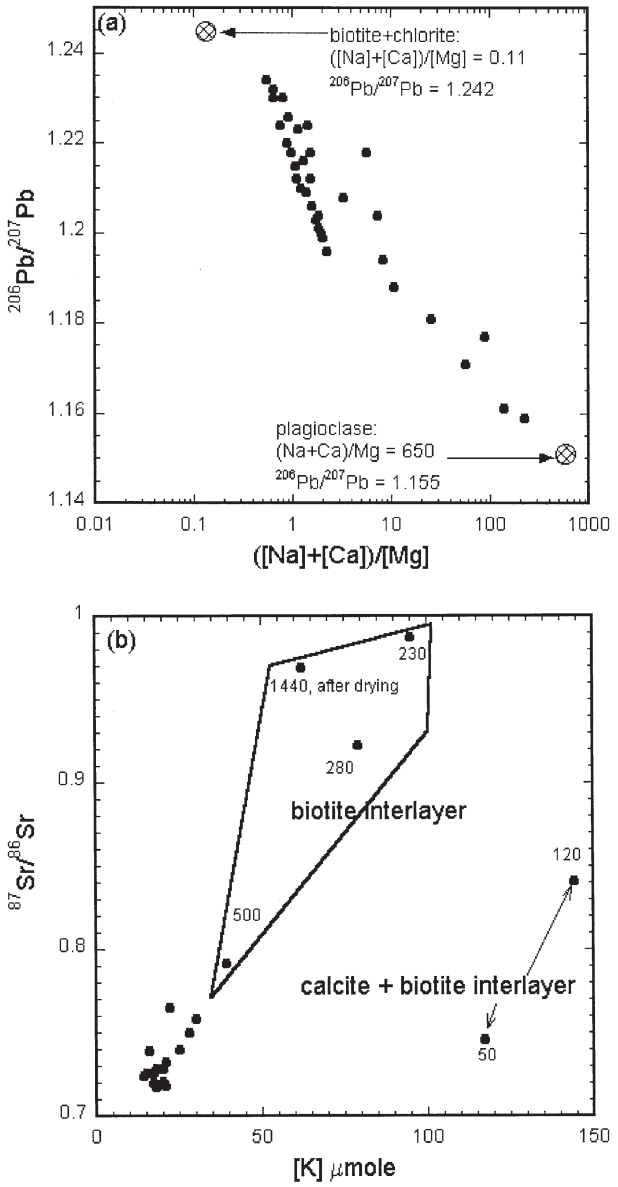

Fig. 5. (a) $^{206}Pb/^{207}Pb$ vs. ([Ca]+[Na])/[Mg] in the effluent solutions of the whole rock dissolution experiment. (b) $^{87}Sr/^{86}Sr$ vs. [K] in the effluent solutions of the whole rock dissolution experiment (numbers indicate time [hours] from the beginning of the experiment).

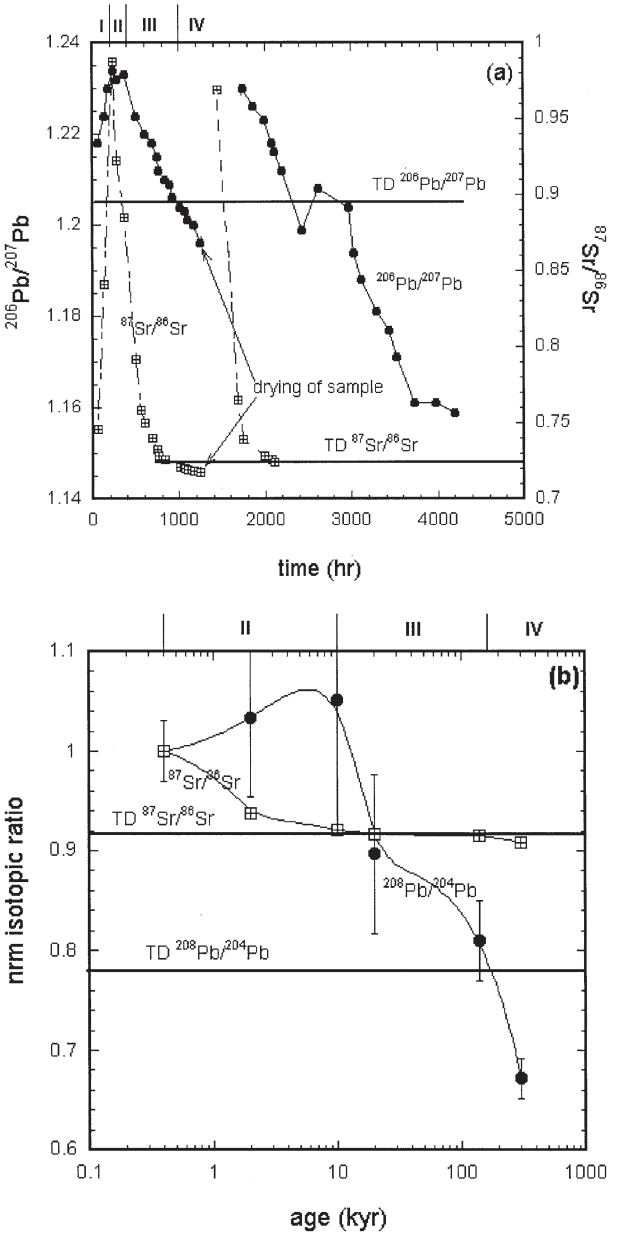

Fig. 6. (a) $^{206}Pb/^{207}Pb$ and $^{87}Sr/^{86}Sr$ values in whole rock sample released to solution as a function of time. The horizontal lines represent the values of the total digests of the whole rock sample. The four dissolution stages I–IV are marked. They are defined as follows: I = increase in $^{206}Pb/^{207}Pb$ and $^{87}Sr/^{86}Sr$ values as a function of time (0–200 h); II = decrease in $^{87}Sr/^{86}Sr$ but not in $^{206}Pb/^{207}Pb$ values with time (200–400 h); III = decrease in both values with time, but still above the total digested rock values (400–1000 h); IV = decrease in both values with time, below the total digested rock values (>1000 h). (b) Normalized $^{208}Pb/^{204}Pb$ and $^{87}Sr/^{86}Sr$ values in the labile fraction of soils from the Wind River Mountains, Wyoming as a function of time. Note the logarithmic scale of the age axis. The horizontal lines represent the average values of the total digests of the whole soil sample. Stage I is missing. II = decrease in $^{87}Sr/^{86}Sr$ but not in $^{208}Pb/^{204}Pb$ values with time (400–10^4 yr); III = decrease in both values with time, but still above the total digested rock values (10^4–10^5 yr); IV = decrease in both values with time, below the total digested rock values (>10^5 yr).

leach), on the other hand, began decreasing only after approximately 10,000 yr, and continued to decrease for 100,000 to 300,000 yr (Erel et al., 1994; Harlavan et al., 1998). The soils of the Wind River Mountains, which have developed on glacial moraines of varying ages, contain a variety of granitoid rock-types and their constituent minerals. These include quartz, plagioclase (An_{7-35}), K-feldspar, biotite, hornblende, magnetite, and minor quantities of pyroxene, garnet, apatite, sphene, muscovite, and chlorite (Blum and Erel, 1997). There is a good resemblance between the shifts in Pb and Sr isotope ratios released by weathering in natural soils described above and in our dissolution experiments (Fig. 6a,b). However, the initial stage of the dissolution experiments, before 200 h when both Pb and Sr values increase with time, is not revealed in natural

soil studies because they do not capture this early, short-lived stage of weathering (Fig. 6b). As in previous studies (White et al., 1999; Taylor et al., 2000a,b), we attribute this initial behavior to the dissolution of minute quantities of calcite in the granitoid rocks.

The decrease in $^{87}Sr/^{86}Sr$ with time is observed in soils older than 400 yr and in our experimental solutions after approximately 200 h. After approximately 10,000 yr in soils and 400 h in the experiments, Pb isotope ratios start to decline as a function of time (Fig. 6a,b). As indicated previously, this change can happen in both $^{206}Pb/^{207}Pb$ and $^{208}Pb/^{207}Pb$ ratios depending on the type of the accessory phase inclusions in the major minerals, most importantly inclusions in biotite and plagioclase. After approximately 100,000 yr, Pb isotopes in granitoid soils reach whole rock values. This also occurs after 1000 h of leaching at pH 1 in the dissolution experiments (Fig. 6a,b). Therefore, it is possible to combine the behavior of Pb and Sr isotopes in soils with their behavior during the dissolution of granitoid rock under acidic condition in the laboratory, to obtain a time-dependent mineral dissolution scheme for granitoid rocks. This scheme outlines the timing of the mineralogic control (i.e., calcite, biotite, plagioclase) on the release of several major (Ca, Mg, Na, K, Fe) and minor (Sr, Pb) constituents during rock dissolution. It is clear that there might be elements which are controlled by minerals other than the ones cited here, but they are probably only minor constituents, as the other major elements (Si, Al) are also controlled by the major minerals emphasized in this study (Roueff, 2003; Table 3). In addition, the timing of these weathering stages might change from one location to another with changing climate, topography, parent material, and vegetation. Additional field observations and experimental data are needed to provide a more generalized relationship between relative weathering rates of minerals in the field and in the laboratory and to allow the generalized use of Pb and Sr isotopes in such studies. In addition, it is important to stress the need for a comprehensive understanding of the mineralogy and petrography of the studied rocks, including the characterization of the accessory minerals and their associations with the major minerals. This knowledge is essential for the utilization of Pb and Sr isotopes in weathering studies.

5. CONCLUSIONS

The isotopic compositions of Pb and Sr are used in this study to trace the proportions of the major minerals that are dissolving during granitoid rock dissolution experiments and to provide a methodology for relating the results of low-pH laboratory experiments to natural soil weathering systems. Combining the isotopic data with major element concentrations allows us to achieve this goal. The initial stage of granitoid dissolution (<200 h of leaching) is controlled by the release of several elements from traces of calcite/apatite and, to a lesser extent, from the interlayer sites in biotite. After 200 to 400 h of dissolution, elemental release is dominated by biotite (mostly interlayer sites) and to a lesser extent by plagioclase. The next stage of dissolution behavior, in the 400 to 1000 h time interval, releases elements mainly from biotite and plagioclase. Finally, after 1000 h, plagioclase and to a lesser extent biotite dominate the composition of elements released from the rock. An advantage of Pb and Sr isotopes in this application is that whereas the major element concentrations released by weathering in natural soils can be obscured by secondary mineral precipitation and ion exchange, the Pb and Sr isotope composition in soils is a robust signal even as Pb and Sr concentrations are modified. By comparing our experimental results for Pb and Sr isotopes with field measurements in chronosequences of soils from the Wind River and Sierra Nevada Mountains (USA), we are able to show that similar isotopic patterns appear in both the low pH experiments and in soils formed under natural conditions. Furthermore, our combined dataset enables us to assess the relative weathering rates of minerals of granitoid rocks under natural conditions in mountainous terrains and temperate climates. The dissolution of calcite/apatite and the interlayer sites of biotite might control element release during the first few hundred years of rock weathering. In rock surfaces older than a few hundred years and younger than 10,000 yr, the release of elements from biotite (mostly interlayer sites) controls the flux of elements by granitoid weathering. Rock surfaces between 10,000 and 100,000 yr old release mostly biotite and plagioclase weathering products, where biotite controls the first part of this period and plagioclase dominates the later part. After 100,000 yr, plagioclase and to a lesser extent biotite determine the composition of the weathering products of granitoid rocks.

Acknowledgments—The authors wish to thank L. Halicz, I. Segal, S. Ehrlich, and O. Yoffe of the Geological Survey of Israel, A. Katz of the Hebrew University, and A. Klaue and B. Klaue of the University of Michigan for assistance in Pb and Sr isotope, trace metal, and major element analyses. We also wish to thank A. Zanvilevich, B. Litvinovsky, M. Eyal, and H. Kisch of Ben Gurion University for their assistance with the petrography of the Elat Granite. The authors thank K. Nagi, L. Stillings, and two anonymous reviewers for their useful comments. This research was supported by a United States–Israel Binational Science Foundation (BSF) grant 1999-076-01.

Associate editor: K. Nagy

REFERENCES

Blum J. D. and Erel Y. (1995) A silicate weathering mechanism linking increases in marine $^{87}Sr/^{86}Sr$ with global glaciation. *Nature* **373,** 415–418.

Blum J. D. and Erel Y. (1997) Rb-Sr isotope systematics of a granitic soil chronosequence: The importance of biotite weathering. *Geochim. Cosmochim. Acta* **61,** 3193–3204.

Blum J. D., Erel Y., and Brown K. (1993) $^{87}Sr/^{86}Sr$ ratios of Sierra Nevada stream waters: Implications for relative mineral weathering rates. *Geochim. Cosmochim. Acta* **58,** 5019–5025.

Blum J. D. and Erel Y. (2003). Radiogenic isotopes in weathering and hydrology. In *Surface and Ground Water, Weathering, Erosion and Soils* (ed. J. I. Drever). Elsevier Science. Vol. 5 in *Treatise on Geochemistry* (eds. K. K. Turekian and H. D. Holland).

Brantley S. L., Chesley J. T., and Stillings L. L. (1998) Isotopic ratios and release rates of strontium measured from weathering feldspars. *Geochim. Cosmochim. Acta* **62,** 1493–1500.

Bullen T. D. and Kendall C. (1998) Tracing of weathering reactions and water flowpaths: A multi-isotope approach. In *Isotope Tracers in Catchment Hydrology* (eds. C. Kendall and J. J. McDonnell), pp. 611–646. Elsevier Science B. V., Amsterdam.

Bullen T. D., White A. F., Blum A. E., Harden J., and Schultz M. S. (1997) Chemical weathering of a soil chronosequence on granitoid alluvium: II Mineralogic and isotopic constraints on the behavior of strontium. *Geochim. Cosmochim. Acta* **61,** 291–306.

Chen J. H. and Moore J. G. (1982) Uranium-lead isotopic ages from the Sierra Nevada Batholith, California. *J. Geophys. Res.* **87** (**B6),** 4761–4784.

Chen J. H. and Tilton G. R. (1991) Applications of lead and strontium isotopic relations to the petrogenisis of granitoid rocks, central Sierra Nevada batholith, CA. *Bull. Geol. Soc. Am.* **103,** 439–447.

Erel Y., Harlavan Y., and Blum J. D. (1994) Lead isotope systematics of granitiod weathering. *Geochim. Cosmochim. Acta* **58,** 5299–5306.

Ganor J., Roueff E., Erel Y., and Blum J. D. (2004). The dissolution kinetics of a granite and its minerals: Implications for comparison between laboratory and field dissolution rates. *Geochim. Cosmochim. Acta* (in press)

Harlavan Y., Erel Y., and Blum J. D. (1998) Systematic changes in lead isotopic composition with soil age in glacial granitic terrains. *Geochim. Cosmochim. Acta* **62,** 33–46.

Harlavan Y. and Erel Y. (2002) The Release of Pb and REE from granitoids by the dissolution of accessory phases. *Geochim. Cosmochim. Acta* **66,** 837–848.

Jacobson A. D., Blum J. D., Chamberlain C. P., Craw D., and Koons P. O. (2002). Climatic versus tectonic controls on weathering in the New Zealand Southern Alps. *Geochim. Cosmochim. Acta* **66,** 3417–3429.

James E. W. (1992) Cretaceous metamorphism and plutonism in the Santa Cruz Mountains, Salinian Block, California, and correlation with the southernmost Sierra Nevada. *Geol. Soc. Am. Bull.* **104,** 1326–1339.

Mattinson J. M. (1978) Age, origin and thermal histories of some plutonic rocks from the Salinian Block of California. *Contrib. Mineral. Petrol.* **67,** 233–245.

Roueff E. 2003. The change in the isotopic composition of Pb and concentration of major elements during the dissolution of Elat granite and their constituent minerals. M.Sc. thesis, Ben Gurion University of the Negev(English abstract).

Sorenson C. J (1986) Soils map of the Fremont Lake South Sublette County, Wyoming. *U.S. Geological Survey*(Map I-1800), scale 1:24,000.

Taylor A. S., Blum J. D., Lasaga A. C., and MacInnis I. N. (2000a). Kinetics of dissolution and Sr release during biotite and phlogopite weathering. *Geochim. Cosmochim. Acta* **64,** 1191–1208.

Taylor A. S., Blum J. D., and Lasaga A. C. (2000b). The dependence of labradorite dissolution and Sr isotope release rates on solution saturation state. *Geochim. Cosmochim. Acta* **64,** 2389–2400.

White A. F. and Blum A. E. (1995) Effects of climate on chemical weathering in watersheds. *Geochim. Cosmochim. Acta* **59,** 1729–1747.

White A. F. and Brantley S. L. (1995) Chemical weathering rates of silicate minerals: An overview. In *Chemical Weathering Rates of Silicates Minerals*, Vol. 31 (eds. A. F. White and S. L. Brantley), pp. 1–21. Am. Mineral. Soc.

White A. F. and Brantley S. L. (2003). The effect of time on the weathering of silicate minerals: Why do weathering rates differ in the laboratory and field? *Chem. Geol.* **202,** 479–506.

White A. F., Blum A. E., Bullen T. D., Vivit D. V., Schultz M. S., and Fitzpatrick J. (1999) The effect of temperature on experimental and natural weathering rates of granitoid rocks. *Geochim. Cosmochim. Acta* **63,** 3277–3291.